

Review

An Overview of Position Sensorless Techniques for Switched Reluctance Machine Systems

Xingtao Tang ¹, Xiaodong Sun ^{1,*} and Ming Yao ^{2,*}

¹ Automotive Engineering Research Institute, Jiangsu University, Zhenjiang 212013, China; 2211904030@stmail.ujs.edu.cn

² School of Automobile and Traffic Engineering, Jiangsu University, Zhenjiang 212013, China

* Correspondence: xdsun@ujs.edu.cn (X.S.); ymluck@ujs.edu.cn (M.Y.); Tel.: +86-0511-8878-2845 (X.S.)

Abstract: Accurate real-time rotor position is indispensable for switched reluctance motors (SRM) speed and torque control. Traditional position sensors add complexity and potential failure risk to the system. Owing to the added advantages of high stability and low cost, the position sensorless method of SRMs has been extensively studied to advance its use in vehicles and construction machinery. This paper presents an overview of position sensorless control techniques from the perspective of whether the method requires the establishment of complex mathematical models. Various types of methods are compared for performance, such as speed regulation range, algorithm complexity, and requirement of the pre-stored parameter. A discussion is presented concerning current trends in technological development, which will facilitate the research addressing potentially effective methods for position estimation in SRM drive systems.

Keywords: additional components; hybrid detection method; position sensorless control; magnetic-model-based; switched reluctance machine (SRM)



Citation: Tang, X.; Sun, X.; Yao, M. An Overview of Position Sensorless Techniques for Switched Reluctance Machine Systems. *Appl. Sci.* **2022**, *12*, 3616. <https://doi.org/10.3390/app12073616>

Academic Editor: Adel Razek

Received: 6 March 2022

Accepted: 30 March 2022

Published: 2 April 2022

Publisher's Note: MDPI stays neutral with regard to jurisdictional claims in published maps and institutional affiliations.



Copyright: © 2022 by the authors. Licensee MDPI, Basel, Switzerland. This article is an open access article distributed under the terms and conditions of the Creative Commons Attribution (CC BY) license (<https://creativecommons.org/licenses/by/4.0/>).

1. Introduction

The switched reluctance motor (SRM) is considered to be one of the best potential motors due to its simple structure, high efficiency, outstanding fault tolerance, and flexible control methods [1–5]. It limits general application in that its doubly salient structure leads to large torque ripple and noise. However, with the rapid development of control theory, finite element analysis (FEA), and power electronics, SRMs are gradually being used in vehicles and other fields [5–10].

At present, switched reluctance motors are widely used in many industrial fields, such as mild-hybrid BSG drives, hybrid vehicles, construction machinery, and aerospace engines, etc., [11–16]. To fully discover the potential advantages of SRM, fault-tolerant control research [17–20], global optimization considering driving cycles and manufacturing fluctuations [21–25], minimum torque ripple control [26–29], and position sensorless control [30–34] have all been extensively studied. The sensorless approach has attracted much attention because it enables the SRM to have the advantages of low cost, low risk, and is not limited by hardware.

For the SRM drive system, the position signal of the rotor is indispensable. However, the position sensor carries a potential risk of failure and limits the speed regulation performance due to the limitation of the sensor resolution [35–45]. To eliminate the negative effects, increasing position sensorless methods have emerged with the deepening of theoretical research on SRMs. As shown in Figure 1, the number of published articles on SRM position sensorless methods is increasing. We have to admit that this is a hot spot, and it is necessary to analyze and review the related theories and technologies.

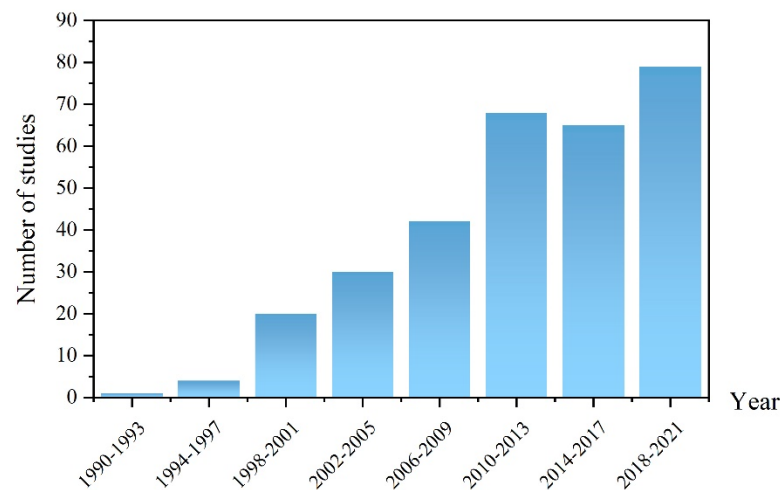


Figure 1. Number of studies published before Jan. 2021 that experimentally examined the position sensorless methods for SRM.

We collected the research to complete our review via a search of ISI Web of Science up to December 2021. The following Boolean search terms and modifiers were employed: switched reluctance *AND sensorless OR position estimation. This initial search yielded 432 papers. Articles were limited to peer-reviewed journal articles in English. Titles and abstracts were read to narrow the list of studies and ensure they met the following criteria: the study had to be an experimental manipulation under field or laboratory conditions linking SRM. Finally, according to these criteria, 311 studies were retained for our systematic review.

Current signal, rotor position, and voltage signal are important feedback signals in the control of SRM drive system. The waveform of the current is especially important for speed/torque control [46–49] and position sensorless control [50,51]. In different speed ranges, the current output of the motor is very different. As the speed of the output increases, the current gradually enters the form of a single pulse. At low speed, the current will be chopped, and the output of torque and rotational speed will be controlled by controlling the range of the chopper. In the medium and high speed segments, the motor needs to output higher power, and the effective value of the current needs to be increased. The motor will control the output of speed and torque by controlling the turn-on angle and turn-off angle, i.e., control the power output by the motor.

Position sensorless technology has attracted much attention and has been widely studied. Such technology can improve the stability of switched reluctance motors to adapt to complex application environments. The sensorless technology has been rapidly promoted via the development of power electronics technology, finite element simulation technology [39–43], flux linkage measurement methods, and control theory. New position sensorless methods are constantly being proposed, which is more coincidental with the requirements of higher position detection accuracy, wider speed regulation range, and better versatility [52–62].

Figure 2 shows the classification of position sensorless methods. In this paper, the classification is based on whether or not the methods require a priori parameters of the motor to build a model. Position sensorless methods are mainly divided into three broad categories: magnetic model-based methods [63–128], magnetic model-free methods [129–149], and hybrid detection methods [150–166]. These methods have their own unique advantages, which are driving the sensorless technology to be more efficient.

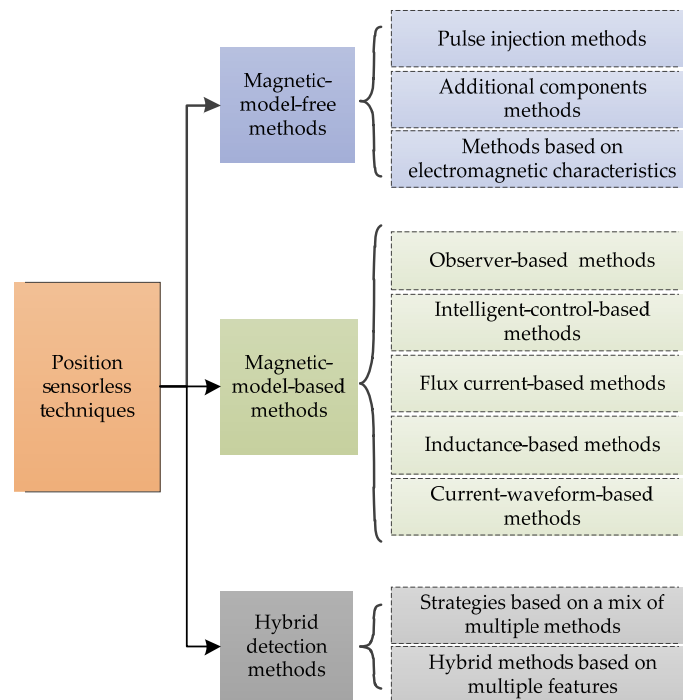


Figure 2. Classification of control methods of position sensorless.

The main work of this paper is to sort out the rotor position estimation method of SRM from the perspective of technology development. The main contribution is to classify different types of sensorless methods and summarize them, demonstrate the process of development of sensorless methods, and essentially explore and categorize a multitude of methods. A comparative analysis is made addressing the feasibility, generality, and speed regulation range of these methods. The sensorless methods with outstanding performance and future research directions are screened out.

2. The Composition of SRM Drive System

2.1. Structure of an SRM System

A typical SRM drive system, shown in Figure 3, is composed of a controller, inverter, motor body, power supply, and various sensors. The motor converts the electric energy provided by the DC power supply into mechanical energy to drive the load. The controller generates the corresponding driving signal through the feedback signal of the sensor to control the motion state of the motor. It is extremely important to detect accurate and effective rotor position signals for SRM control. The position sensorless method can significantly increase the stability of the system. These methods estimate the rotor position by adding hardware, a magnetic model, or control algorithm.

The converter is important to the SRM system because of the sampling of phase current, bus current, and phase voltage. As shown in Figure 4, the A phase of the three-phase half-bridge converter is used as an example to illustrate the process of converter operation. Figure 4a is the circuit topology of a single-phase half-bridge, which consists of two controlled switches, S_{A1} and S_{A2} , and two diodes, D_{A1} and D_{A2} . The converter has three modes: magnetization, zero freewheeling, and demagnetization. As shown in Figure 4b, when winding A needs to establish a magnetic field, S_{A1} and S_{A2} are turned on. In the freewheeling mode, only S_{A1} or S_{A2} is turned on, as shown in Figure 4c. When winding A no longer needs to establish a magnetic field, S_{A1} and S_{A2} are turned off at the same time, which will force the current commutation of winding A to achieve the purpose of eliminating the magnetic field. Meanwhile, the voltage across the winding is the negative phase voltage $-U_{dc}$.

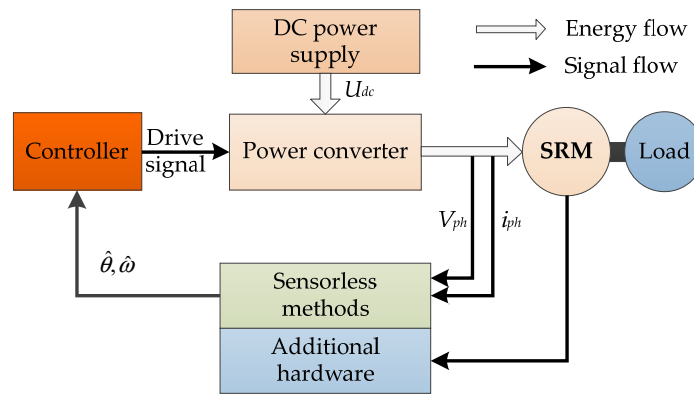


Figure 3. The structure of position sensorless SRM drive system.

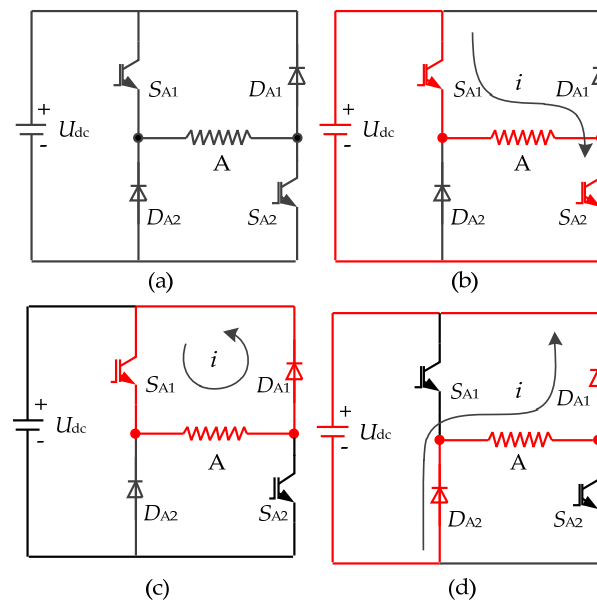


Figure 4. Topology of asymmetric half-bridge inverter. (a) Static structure. (b) Magnetization. (c) Freewheeling. (d) Demagnetization.

2.2. Mathematical Model of SRM

The motion state of the SRM can be controlled as long as the windings of each phase are driven according to certain principles. Figure 5 shows the change of the electromagnetic state of a 12/8 three-phase SRM during the rotation of one rotor pole pitch. The first state is that the salient poles of the rotor are aligned with the center of the grooves of the stator as shown in Figure 5a. The rotor turns 22.5° counterclockwise to reach the second state. At this time, the rotor salient poles are aligned with the center of the stator salient poles. In [0°, 22.5°], the inductance of this phase gradually increases from minimum to maximum due to the decrease in reluctance. After that, the inductance will decrease until it turns another 22.5° to reach the third state. As shown in Figure 5b,c, the static curves of flux linkage and torque under different currents can be obtained by finite element analysis.

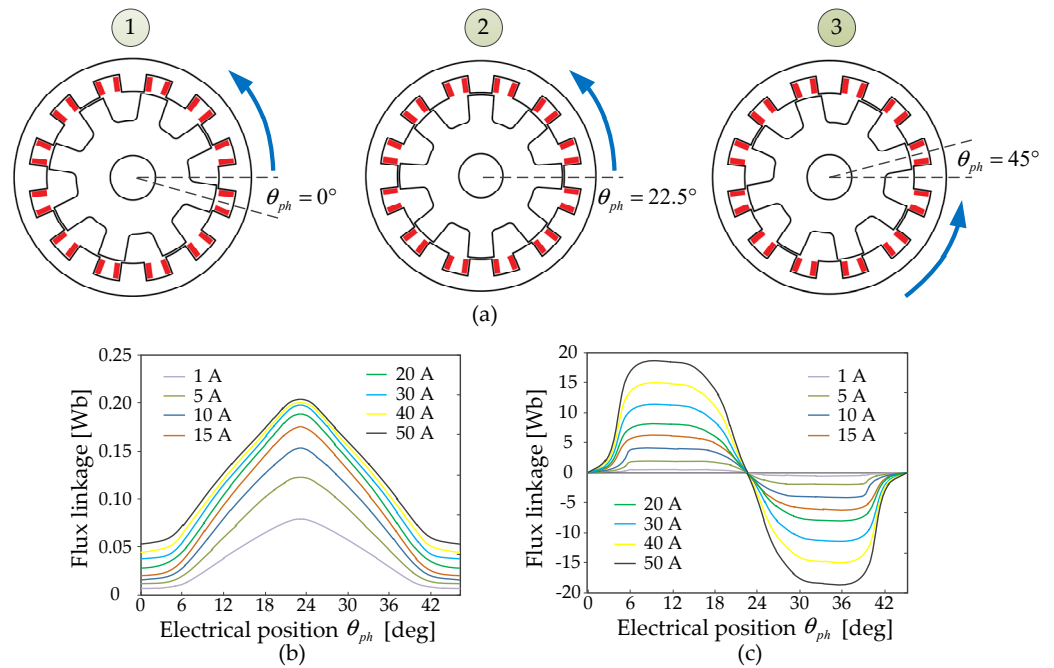


Figure 5. SRM structure topology of a three-phase 12/8 poles and electromagnetic properties. (a) Rotor electrical angle. (b) Magnetization curve. (c) Phase torque curve.

The motor conforms to the law of electromagnetic induction in the process of operation. The motor has m phases, and each phase winding satisfies Equation (1). As shown in Figure 5, the flux linkage of SRM is very nonlinear due to its structure. The flux linkage model can be fitted mathematically, but the accuracy of this method is greatly limited. Generally, the magnetic link information is obtained by the three-dimensional look-up table (LUT) method.

$$e_k = -\frac{d\psi_k}{dt} \tag{1}$$

where ψ_k , e_k , and t represent the flux linkage, induced electromotive force, and time of the k th phase winding, respectively, and $k = 1, 2, \dots, m$.

There is a mapping relationship between the flux linkage ψ_k , the rotor position angle θ_{ph} , and the phase current i_k . The relationship between the flux linkage and the inductance L_k is shown in the following formula.

$$\psi_k(\theta_{ph}, i_k) = L_k(\theta_{ph}, i_k) i_k \tag{2}$$

where L_k and i_k represent the phase inductance and phase current, respectively. θ_{ph} is rotor position.

According to Kirchhoff's voltage law, each phase loop conforms the voltage balance equation.

$$U_k = R_k i_k + \frac{d(i_k \cdot L_k)}{dt} \tag{3}$$

where U_k and R_k represent the phase voltage and phase resistance, respectively.

The mechanical balance equation can be obtained via the relevant mechanics theory.

$$T_e = J \frac{d\omega}{dt} + T_L + D\omega \tag{4}$$

where T_e and T_L represent the electromagnetic torque generated by the motor and load torque, respectively. J and D are the const parameters of the moment of inertia and viscous friction coefficient. ω is the actual speed of the motor.

The relationship between these physical quantities is the basis of the control research for SRM, not only for the rotor position estimation control, but also the design of the motion control algorithm [52,53]. The speed control algorithm determines the output performance of the motor, including torque quality, speed regulation range, and robustness. Common speed control methods include current chopping control (CCC), angle position control (APC), voltage chopping control (VCC) [54–57], direct torque control (DTC) [58,59], and direct instantaneous torque control based on torque sharing function (TSF) [60–62]. Another type of control algorithm is the signal fault tolerant and position sensorless control algorithm, which is designed to enhance the stability of the hardware layer. There is an inevitable connection between speed control and position-free fault-tolerant control. The position sensorless control provides the rotor position signal for the control algorithm, and the control algorithm can also provide the required physical quantities for some rotor position estimation methods.

Meanwhile, we can discover new methods in these essential electromagnetic and mechanical equations to improve the performance of the motor drive system, which will be reflected in many position estimation methods. The most closely related to the rotor position is the flux linkage and inductance, which motivates a large number of magnetic-model-based methods. At the same time, the magnetic-model-based method is also undergoing in-depth development to solve the difficulty involved in magnetic model establishment.

3. An Overview of Recent Development in Position Estimation Methods of SRM

We have reviewed related methods to facilitate a clear understanding of the development of different methods so that we can find some characteristics and future development directions of position estimation. We will introduce various categories of position estimation methods, which are selected from papers with experimental result verification, and can quantify the performance of the method, such as speed regulation range or estimation error.

3.1. Magnetic-Model-Based Position Sensorless Methods

Equation (2) shows that the rotor position estimation has a direct mapping relationship to flux-current and torque-current. A large number of methods have been proposed based on magnetic models and magnetic equations [44].

3.1.1. Based on Flux-Current-Position Methods

There is a mapping relationship between the rotor position and the flux-linkage-current, which determines that this is a direct and effective rotor position direction. This kind of method consists in using various features to generate new flux-linkage-based methods, on the one hand building more accurate models, and on the other hand using fewer prior parameters to reduce pre-storage.

During the operation, the calculation of the flux linkage satisfies the following Formula (5).

$$\psi_k(t) = \psi_k(0) + \int_0^t (U_k - R_k i_k) dt \quad (5)$$

where $\psi_k(0)$ represents the flux linkage value at the initial moment.

Methods based on 3D LUT [63–65] and flux linkage modeling [66–73] are used to obtain the position signal by obtaining current and flux linkage information. Then, to gradually reduce the dependence on the pre-storage, the magnetic characteristics, such as the flux linkage and inductance increment of the SRM, are decomposed into the rotor position and the appropriate amount of phase current, and a one-to-one correspondence between the flux linkage and the rotor position can be established. The position estimation is carried out within the wide speed range. However, the dependence on speed and torque control strategy is extremely strong [74,75]. Using only a one-phase current sensor and virtual voltage to build a flux linkage model to estimate the rotor position can perform rotor position estimation in a wide speed range [76]. However, the stability of the method is worth exploring due to the severe nonlinearity of the flux linkage.

On the other hand, to compensate for the limitation brought by model accuracy, based on numerical method [77,78], quadrature flux estimators [79], Kriging interpolation model [125], and compensation error method are used. Recently, the accuracy of the method has been further improved by eliminating the errors of the flux linkage modeling by compensating errors online and estimating the winding resistances [80,81]. The accuracy of position estimation is enhanced by the special flux linkage curve of position [82–84]. These methods indirectly contribute to the accuracy of rotor position estimation.

3.1.2. Based on the Inductance Model Methods

Inductance and flux linkage are the same as the most important essential characteristics of electric machines. Therefore, they have been extensively studied to promote the development of indirect position estimation. The calculation of the inductance has a simpler calculation method than the flux linkage, as can be seen from Equation (3). Inductance has a direct balance relationship with voltage and current, so various inductance-based methods have been proposed. These methods are intensively studied in inductance modeling, inductance acquisition methods, and considering the inductance–position relationship to indirectly obtain the rotor position.

As shown in Figure 6, the phase inductance is the largest at the aligned position θ_a of the stator and the rotor and the smallest at the misaligned position θ_u . Generally, three special positions are selected for parameter fitting to establish a mathematical model of the inductance. The inductance model based on the Fourier series is shown in (6).

$$L_k(\theta_{ph}, i_k) = L_0(i_k) + L_1(i_k) \cos(N_r\theta_{ph}) + L_2(i_k) \cos(2N_r\theta_{ph}) \quad (6)$$

where L_0 , L_1 , and L_2 are the parameters to be fitted and N_r represents the number of rotor poles.

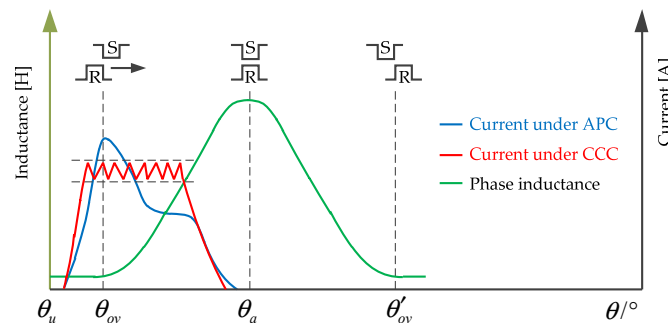


Figure 6. Current waveforms for different control algorithms and inductor cycles.

Based on the inductance model of first switching harmonics via Fourier series to reduce the need for controller memory and interpolation [85,86]. The online calibration [87,88], considering mutual inductance [89], and considering magnetic saturation [90,91] were used to enhance the accuracy of the inductance model.

In terms of the method of inductance acquisition, the rotor estimation method based on the inductance modeling-current model is incremental inductance [92] utilizing the conduction phase measurement, and the motor performs well in the low speed range. Phase inductance information is obtained based on pulse injection, and then the combined vector quadrature decomposition method is combined with the inductance partition method to eliminate position sensors [93]. Further, many scholars have found various relationships between the inductance characteristics and the rotor position to effectively detect the rotor position. After rotor position failures are detected, an inductance slope-based method is used to supplement the missing signal [94,95]. After that, a method based on phase-inductance vector coordinate transformation was proposed and improved [96,97]. Unbalanced inductance will cause the traditional inductance feature-based and inductance modeling-based methods to reduce the accuracy of position estimation, and even fail to

drive the motor, as shown in Figure 7. Further, to improve the general applicability of rotor position estimation, a detection method considering inductance imbalance is applied [98]. As shown in (7), by establishing the relationship between the inductance and the current, the zero-crossing law of the slope at the inflection point of the inductance can be found [99–101]. Such a feature is efficient for localization of the rotor position θ_{ov} without the need for additional sensors and additional circuitry.

$$\begin{cases} U_{0-} = \omega L_{0-} \frac{di_{0-}}{d\theta_{ph}} + \omega i_{0-} \frac{dL_{0-}}{d\theta_{ph}} \\ U_{0+} = \omega L_{0+} \frac{di_{0+}}{d\theta_{ph}} + \omega i_{0+} \frac{dL_{0+}}{d\theta_{ph}} \end{cases} \quad (7)$$

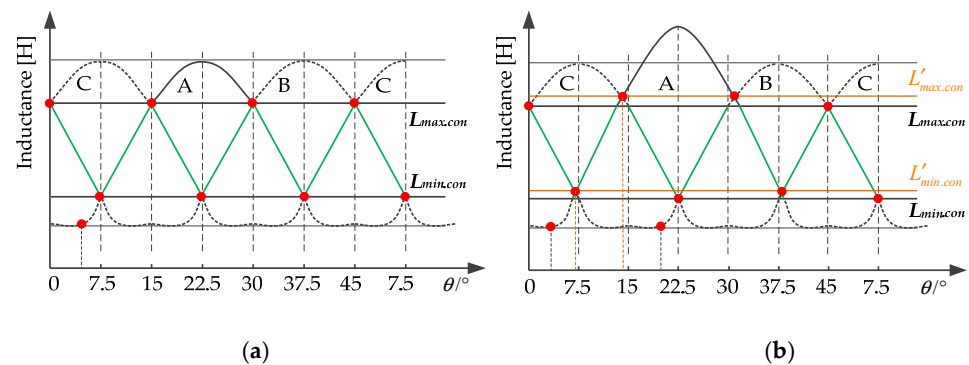


Figure 7. Phase inductance curve of a 12/8 three-phase SRM. (a) Balanced inductors. (b) unbalanced inductors.

3.1.3. Based on Intelligent Control Algorithm

Intelligent control algorithms have outstanding performance in dealing with non-linearity [102–104]. For the position estimation of SRM, the advantage of this type of algorithm is that the nonlinear modeling of flux linkage and inductance is accurate, and the disadvantage is that the algorithm is difficult to design and needs to measure a large number of motor parameters.

In [105–107], the fuzzy logic control algorithm replaces the traditional three-dimensional look-up table method and mathematical modeling method. This reduces the amount of pre-stored data. Figure 8 shows the rotor position estimation scheme based on the principle of the neural network. Complicated fuzzy rules and complex offline training limit its use. Figure 8a shows the block diagram of the neural network application, which takes the phase current and phase voltage as input, calculates the rotor position, and then outputs it. The input layer, hidden layer, and output layer constitute a functional neural network, as shown in Figure 8b. A neural network is trained based on the relationship between flux linkage and current position to form a nonlinear SRM mapping relationship [108–111]. The established neural network model only needs to use the sampled current/voltage for rotor position estimation [112]. After that, the neural network is improved to improve the performance of rotor estimation, such as back-propagation neural network (BPNN), by adding a pretreatment section that refines the input layer to improve performance [113]. Although neural networks have outstanding advantages in terms of model accuracy, they all require a large number of actual measurement data samples to have sufficient accuracy.

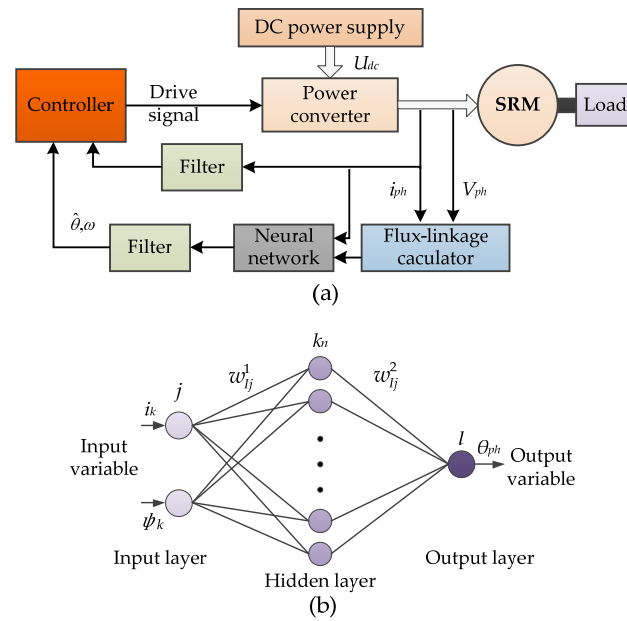


Figure 8. Rotor position estimation principle based on neural network (a) Block diagram of SRM sensorless system based on neural network. (b) Artificial neural networks.

3.1.4. Observer-Based Methods

Compared with intelligent algorithms, the development of modern control theory provides a new method of position control. The state equation of the system can be established, and the observer can be constructed to measure the physical quantity that is not convenient to measure directly. The flux observers, position observers, and sliding mode observers are also used to obtain the rotor position indirectly [114–117]. Generally, such algorithms have the advantages of torque- and speed-independent control algorithms, no pre-stored large amounts of data, and wide applicability to speeds. More deeply, this kind of position estimation control needs to set more parameters, which is its disadvantage.

$$\begin{cases} \frac{d\psi_k}{dt} = -R_k i_k + U_k \\ \frac{d\omega}{dt} = -\frac{1}{J} D\omega - \frac{1}{2J} \psi_k^T \frac{d\mathbf{L}_k^{-1}(\theta_{ph})}{d\theta_{ph}} \psi_k \\ \frac{d\theta_{ph}}{dt} = \omega \\ i_k = \mathbf{L}_k^{-1}(\theta_{ph}) \psi_k \end{cases} \quad (8)$$

where J and D are the moment of inertia and viscous friction coefficient of the motor, respectively. ω is the rotational speed.

The basic equations satisfied by the SRM system are shown in (8). Hence, many studies will design different observers based on different control theories, such as sliding mode control and nonlinear state observers. This class of position sensorless methods is an application of modern control theory [37,118]. The performance of advanced control algorithms is highlighted in the efficient aspects of speed regulation, torque regulation, and position estimation [118].

Based on the general nonlinear magnetizing model (GNMM) was applied to estimate the rotational speed and the position of the rotor [127]. With the introduction and development of sliding mode control theory, sliding mode observers have been designed and improved to improve performance [121–126]. Early position estimation methods based on sliding mode observers used linear models, which limited their accuracy. With finite element modeling and nonlinear fitting improving the accuracy of flux linkage and torque calculations, a second-order inductance model based on the Fourier model is used in a typical second order sliding-mode observer to observe the rotor position. Later, scholars improved the performance by improving the approach control law to force the rotor posi-

tion estimation error to converge to the sliding mode surface [124,126]. In order to solve the rotor position error caused by nonideal measurement noises and flux linkage calculation errors, as shown in Figure 9a, a nonlinear state observer (NSO) is designed to indirectly measure the rotor position with special position detection. In addition, a comparison between the linear observer and the proposed observations was made in terms of position estimation and speed estimation, as shown in Figure 9b [128]. The observer has outstanding performance in the medium- and high-speed range. The observer design is also more difficult, but it can reduce the need for motor parameters and is not limited by the speed range. The discovery of modern control theory is a direction full of potential opportunities.

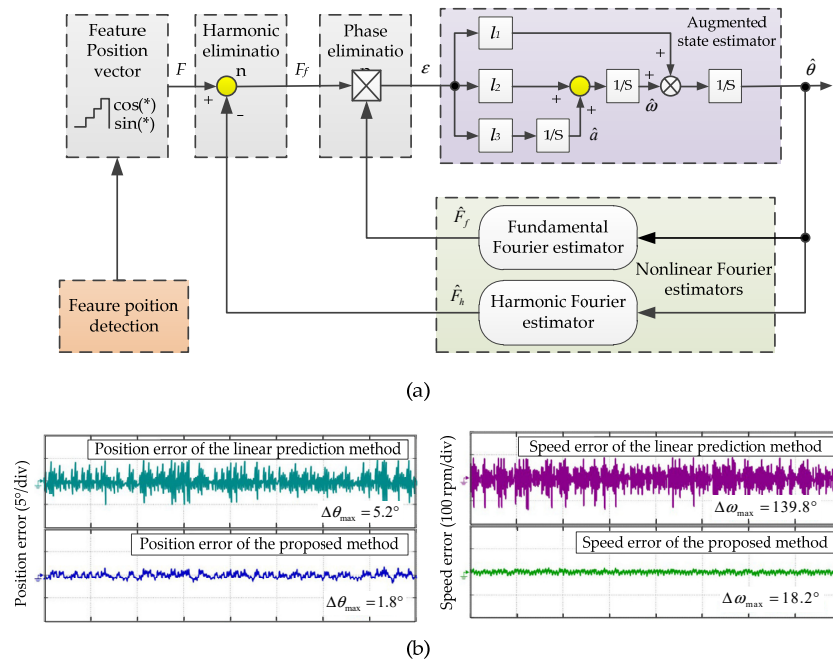


Figure 9. The principle block diagram of observer-based position sensorless control. (a) Observer (b) Contrast experiment [128].

Methods that require the use of electromagnetic quantities are the most mentioned. It is obvious that this is an important direction for the future development of location-free methods. Through the above introduction, Table 1 shows the characteristics of these types, the current development, and the future development direction. The observer advantage here is huge due to the speed-independent torque control strategy. Due to the complex design of the artificial intelligence algorithm, it does not have an obvious advantage in rotor position estimation.

Table 1. Prediction of the development of existing methods.

Methods	Versatility	Improved	Future
Based on flux-current-position method	CCC, APC and VCC	Reduced pre-stored parameters	increase general Versatility
Based on flux-current-position method	CCC, APC, VCC and TSF	Inductance characteristics are fully utilized	Enhance real-time
Based on intelligent control methods	ALL	Improve neural network structure	Reduce complexity
Observer-based methods	ALL	Adopt the observer with strong anti-interference	Effectiveness at low speed

3.2. Magnetic-Model-Free Method Position Sensorless Methods

To decouple the rotor position from the flux linkage/inductance, some methods without the use of models are proposed for various speed and torque control strategies and without pre-stored flux linkage/inductance.

3.2.1. Additional Component-Based Methods

A circuit is designed to measure the voltage required for rotor position estimation, and the rotor position can still be estimated under the premise of considering self-inductance and inductance. The resonant circuit has a good real-time rotor position estimation, calculated as the resonance peak as shown in (9) [139]. However, the real-time performance of the rotor position is not ideal. To reduce the predefined inductance parameters, the method based on the bootstrap circuit using bootstrap circuit can effectively detect the initial position of the rotor [140,141].

$$U_R = \frac{U_k}{1 + jQ[(f_1/f_0)^2 - 1]} \tag{9}$$

where $f_0 = 1/(2\pi\sqrt{LC})$, $Q = 1/(2\pi f_1 RC)$, R and C represent the resistance and capacitance in the circuit respectively, and L is the inductance of the characteristic position in the motor.

As shown in Figure 10, a method based on series inductive coils was proposed [142]. The excitation winding detection coils are independently wound on the stator teeth. According to the different structure of the winding, there are three structures, NNNN, NNSS, NX SX, which are designed to estimate the position of the rotor with the corresponding signal conditioning circuit. Since it is not affected by the winding, this method has the advantages of high detection accuracy, independent control algorithm, and wide speed range. However, it will also increase the risk of the system due to the addition of new accessories.

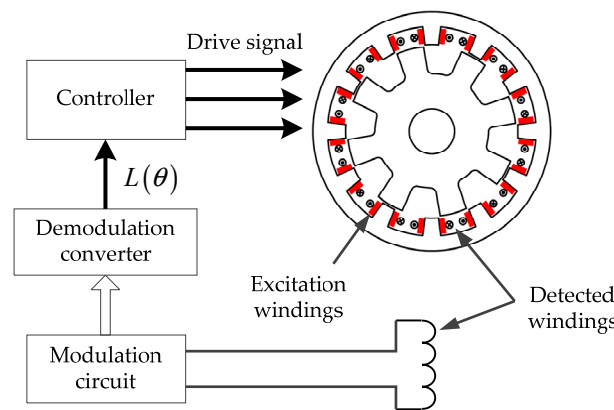


Figure 10. Position estimation method based on additional windings.

3.2.2. Methods Based on Pulse Injection

The pulse injection method is divided into pulse injection into the excitation phase and pulse injection into the non-conduction phase. The theoretical basis that these methods follow is shown in Formula (10).

$$U_k \approx L(\theta_{ph}) \frac{\Delta i}{\Delta t} \tag{10}$$

where Δi and Δt are the current change rate and time interval of the detection coil, respectively.

The pulse injection method for startup is relatively mature. In [129–132], an initial position estimation method based on non-conducting phase pulse injection was proposed for the first time. To eliminate the start-up hysteresis, a method of injecting short-duration pulses into all phases was proposed [133]. Later, many studies combined current waveforms to achieve operation over a wider speed range. A general low-speed position sensorless

based on the principle of phase-locked loop was proposed [134]. There are few pulse injection methods in the high-speed range, and the pulse injection will affect the torque control of the motor. A single-pulse and integrator circuit was combined to broaden the position estimation, addressing the operating frequency limitations of power devices. Non-operating phase injection pulses was proposed [136]. The required pulses are injected into the motor windings via the existing inverter. High-frequency pulse injection was utilized [131]. Different algorithms are used at different velocity stages.

As shown in Figure 11, a position estimation method based on high frequency sinusoidal signal injection has been proposed [137,138]. The high-frequency sinusoidal signal v_{hf} is superimposed on the driving voltage V_{ref} and compared with the high-frequency triangular wave to generate a SPWM wave signal to drive the inverter, and indirectly obtain the rotor position by responding to the current waveform. No pre-stored magnetic parameters and strong versatility are the advantages of this method. However, the speed regulation range and the execution frequency of power devices represent great challenges for this type of method.

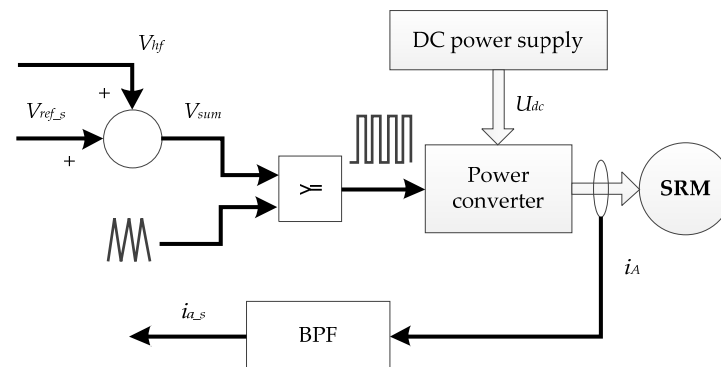


Figure 11. Schematic of the pulse injection method.

3.2.3. Methods Based on Electromagnetic Characteristics

This type of method does not require mathematical modeling or a three-dimensional look-up table like the model-based method, but uses certain characteristics of the motor to perform position detection.

Current is an inescapable variable for all rotor position estimates. The rotor position can be extracted by the characteristics of current, which has a good versatility in low speed and start-up [143]. The critical position is based on the chopping current time width [144], based on the lowest point of the inductance [145], and on the inductance start to rise point [146]. Using the current gradient sensorless (CGS) scheme method [147] of the current slope in the wide speed range, the rotor position estimation performance remains stable. One of the more typical formulas uses the slope of the current to detect the position of the minimum inductance. The basic Equation (7) is satisfied on the left and right sides of the minimum inductance point. Equation (12) is obtained by subtracting (7), and the special point of the inductance is obtained by derivation of the rotor through the current.

$$\frac{di_{0-}}{d\theta_{ph}} - \frac{di_{0+}}{d\theta_{ph}} = i_{0+} \frac{dL_{0+}/d\theta_{ph}}{L_{\min}} > 0 \quad (11)$$

where i_{0-} and L_{0-} represent the current and inductance values approaching the left of the inductance inflection point, respectively. i_{0+} and L_{0+} represent the current and inductance values approaching the right of the inductance inflection point.

The traditional inductance slope zero-crossing detection has a large number of interference signals. The crossing point of motional electromotive force (MEF) and the transformer electromotive force (TEF) are detected as a characteristic position, as shown in Figure 12a. The experimental results in the literature verify the correctness of the principle as shown in

Figure 12b. To use fewer sensors, the bus current is decomposed, and the current gradient is then used to estimate the rotor position [149]. The theoretical basis is to expand Equation (3) to obtain Equation (12).

$$U_k = R_k i_k + L_k \frac{dL_k}{dt} + i_k \frac{d(\cdot L_k)}{dt} = R_k i_k + E_{MEF} + E_{TEF} \tag{12}$$

where E_{MEF} and E_{TEF} represent motional electromotive force and transformer electromotive force, respectively

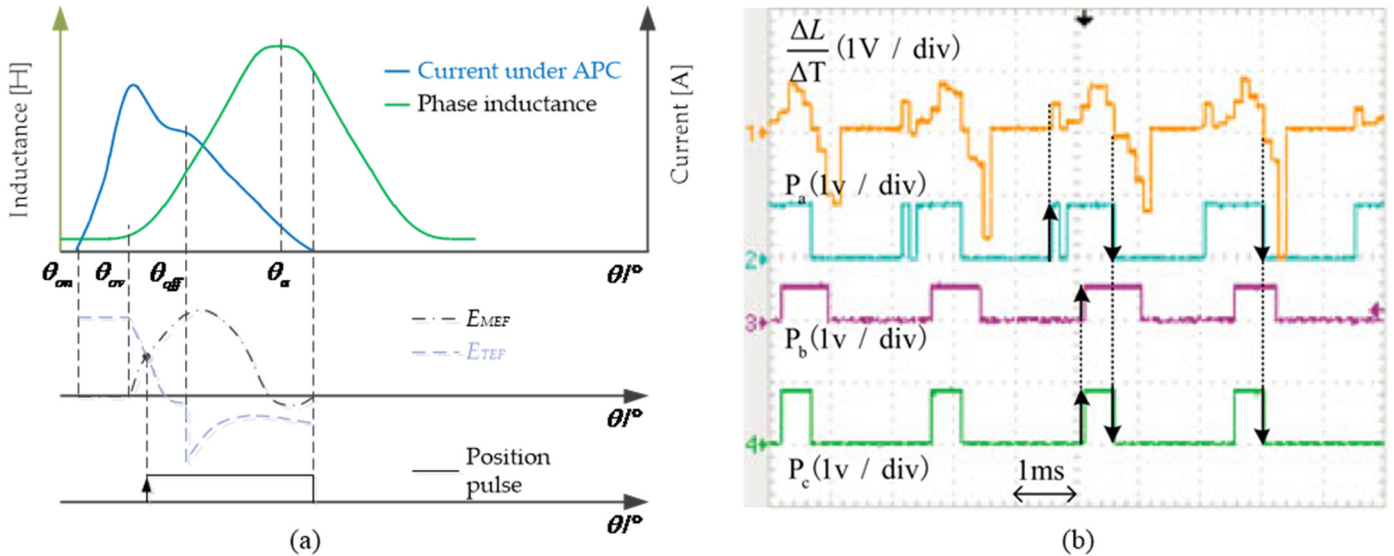


Figure 12. Principle of the crossing point of E_{MEF} and E_{TEF} (a) Principle (b) Experiment [148].

As the rotational speed increases, E_{TEF} much larger than E_{MEF} affects the position-free estimation at high speed. The accuracy of this method is high in the low and medium speed range. The feature point-based method is efficient and, in particular, has good performance in a specific speed range. However, because the position corresponding to the feature quantity is less, this will limit the speed regulation performance and real-time performance of the motor.

3.3. Hybrid Detection Position Sensorless Method

In recent years, a variety of position-free control strategies have been mixed to form a method for full speed range estimation. Such methods combine multiple magnetic features and use different methods for position estimation at different velocity ranges to meet performance.

3.3.1. Strategies Based on a Mix of Multiple Sensorless Approaches for Full Speed Range

Hybrid control algorithms are very common in control because they can comprehensively utilize the advantages of multiple parties [150–153]. Active fault-tolerant techniques are proposed to deal with position sensor failures. The method of pulse injection is applied [155]. This method is the most widely used, and the pulse injection method is cited as the starting method in many approaches [94,148]. Four-phase operation is of great significance for SRM to meet more applications. In [123], a state observer and a pulse injection-based inductance detection method are combined to enable the motor to perform well in the starting and full speed range. Position sensorless methods based on fewer current sensors were proposed [149,153,160]. The main contribution of these methods is to reduce the current sensor, and the position scheme will be based on the characteristics of inductance and current. There are position sensorless control methods for diagnostic fault tolerance after position sensor failure [94,95,101,155].

This type of hybrid rotor position estimation method demonstrates a relatively outstanding performance in the local speed range, but in-depth research on other mature methods directly cited has not been performed. However, how to smoothly connect different methods needs to be paid attention to, especially in the case of sudden load or variable speed conditions.

3.3.2. Hybrid Detection Method Based on Multiple Features

Another hybrid method is to use multiple means to estimate the rotational speed and locate the special position to make up for the shortcomings of the traditional single method. Pulse injection is combined with flux linkage [156,157]. Multiple inductive features [158,159]. Mutual inductance-based methods [164,165] are proposed to obtain the rotor position based on the induced voltage generated by the mutual inductance effect between the motor phases, which is a typical hybrid detection technique. During SRM operation, the mutual inductance voltage is formed between the conducting phase and the non-conducting phase, by detecting the change accompanying the mutual inductance voltage when the rotor position changes. After that, the rotor position is estimated by combining the characteristics of the inductance. However, the back EMF can adversely affect the accuracy of the estimation. In [166], a high frequency pulse is injected into the tail of the excitation current. The current waveform and flux linkage waveform are shown in Figure 13. During the start-up and low-speed phases, the inductance is divided into multiple regions, a linear region of which is selected for rotor position estimation. In the medium and high speed regions, the excitation current flux linkage and the current generated by the injection pulse are compared for rotor positioning. This method enables four-phase operation for the full speed range and start-up phase.

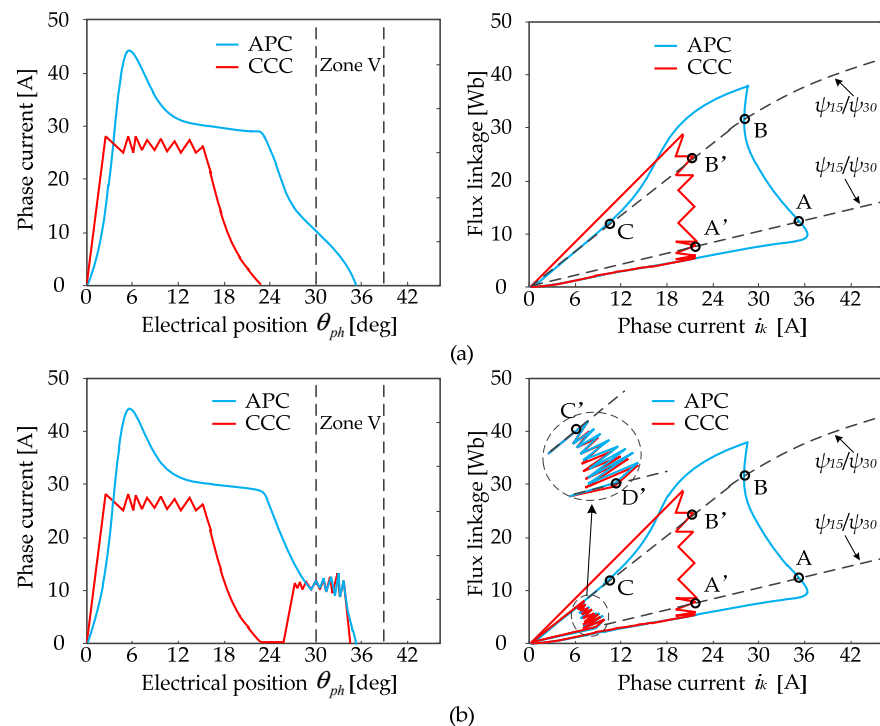


Figure 13. Schematic diagram of the hybrid method based on flux linkage and current waveforms. (a). Normal excitation mode. (b). excitation mode with chopping.

This type of scheme deserves further study, and its unique advantage is that it can make up for the inherent shortcomings of the original method by introducing new methods. It has huge advantages in speed regulation range, four-phase operation, and no pre-stored parameters.

The differences between the various methods can be easily obtained by comparing the Table 2. In general, some methods are effective and widely used in certain speed ranges, e.g., pulse injection in the start-up phase, inductance-based methods in the mid-to-high speed range, and observer-based, add-on-based methods in the full-speed range. In order to find a control strategy without pre-storage, in the full speed range, independent of the speed/torque control strategy and with high position estimation accuracy, it is extremely important to study the electromagnetic characteristics and control theory of the motor to obtain the rotor position signal indirectly.

Table 2. Comparison of the various sensorless methods.

Categories		Speed Range	Pre-Stored Parameters	Advantages	Shortcomings
Pulse injection methods		Startup and low speed	Small	Accurate, easy to implement	Negative torque ripple generation
Additional components methods		Whole-speed	Without	Universal versatility	Introduced new components
Electromagnetic-characteristics-based methods		Whole-speed	Small	Simple, effective and stable	Poor real-time performance
Flux-current-based methods	Traditional	Medium and high speed	Large	Good real-time performance	Poor versatility, huge calculation
	Developed	Whole-speed	Medium	Without additional components	Poor versatility
Inductance-based methods	Traditional	Medium and high speed	Medium	Small amount of computation	Large estimation error, difficult modeling
	Developed	Whole-speed	Medium	Small amount of computation	Poor real-time performance
Intelligent-control-based methods		Whole-speed	Medium	Universal versatility, Good real-time performance	Difficult algorithm design
Observer-based methods		Whole-speed	Without	Good robustness, universal versatility	Poor accuracy in low speed, difficult algorithm design
Strategies based on a mix of multiple methods		Whole-speed	Medium	Accurate location estimation	Requires switching algorithm
Hybrid method based on multiple features		Whole-speed	Small	Various methods, easy to implement	Poor real-time performance

4. Future Directions

By summarizing and reviewing the existing literature, the method of rotor position estimation has been developed rapidly. There are also more requirements for the target of rotor position estimation. In addition to the known position sensorless method to ensure the estimated rotor position is accurate and real-time, there is a deeper understanding such that the development direction focuses on the following aspects.

4.1. An Accurate Rotor Estimation Solution in Whole-Speed Range

Position sensorless technology for the full speed range is an ongoing goal. Many methods demonstrate accurate position estimation in part of the velocity range, which is also of great significance for the development of position sensorless methods. However, this limits the practical application of the algorithm in that the motor is required to be in the full speed range. It is necessary to seek rotor position estimation methods in a wider speed range.

4.2. Reduce Coupling between Position Estimation and Control Methods

For motor motion control, current chopper control (CCC), angle position control (APC), and voltage chopper control (VCC) are relatively mature control algorithms. Many position estimation methods are extremely dependent on these control strategies, which is weak compared with traditional position sensors. Many new controls, such as direct torque con-

trol (DTC) and torque sharing function (TSF) [154,160–162], have outstanding performance in reducing torque ripple and vibration noise, and the current waveforms produced by these methods are completely different due to different control strategies [134,135]. This forces the position estimation methods to be able to adapt to these new control strategies.

4.3. Reduce the Need for Prior Parameter Storage

The gradual reduction of the motor a priori parameter requirements can reduce the pressure on microcontrollers with small storage capacity. Of course, we also have to realize that some key motor parameters are instructive for estimating rotor position. The validation of prior parameters restricts the application of location-free methods to SRMs with large parameter differences. Moreover, many motor parameters may be changed by the interference from the environment and working conditions, which is a huge risk to the long-term effectiveness of the algorithm.

4.4. Smooth Switching between Different Speed Stages

The motion process of conventional SRM is mainly divided into the start-up, low-speed, and high-speed stages. How to effectively switch between different sensorless methods is a technical point worth paying attention to [166]. For example, in [133], the pulse injection method is combined as the algorithm for the start-up phase. However, it does not indicate how to switch.

4.5. High Stability under Heavy and Changing Loads

It is well known that drastic changes in load can challenge the robustness of the control algorithm. In the experiments of some literature, it is easy to observe that the estimation accuracy will be lower than the light load when the load is abruptly changed. How to effectively improve the accuracy of rotor position estimation is a worthy research direction under various working conditions.

The principles of various types of sensorless methods have been introduced in detail, and their development has been teased out. The direction of the entire sensorless development is elucidated based on the current development direction. It is important to see what changes can be made in the future for each type of method. Table 3 presents future applications and future developments of the various methods summarized. From a practical application point of view, hybrid and observer-based methods enable a decoupling of speed/torque control strategies and position estimation in the full speed range.

Table 3. Prediction of the development of existing methods.

Methods	Features of Application	Future Development
Pulse injection methods	Outstanding startup performance	Hybrid with other methods
Additional components methods	Similar to the novel position sensor	Smaller additional components
Flux-current-based methods	Excellent real-time performance	More accurate analytical models
Inductance-based methods	Simple detection of special positions	Enhance real-time
Intelligent-control-based methods	For the acquisition of electromagnetic values	Mate position sensorless method
Observer-based methods	Outstanding real-time performance, decoupling from speed control strategy	Improvements at startup and low speed
Hybrid method	Suitable for whole-speed	Smoother mode switching

5. Conclusions

This paper reviewed the developments in the position estimation of SRMs, with a focus on the application of position sensorless methods. Via the discussions, it is found that there are many obvious constraints and potential opportunities for the sensorless technology, with the development of advanced control theory and the in-depth study of electromagnetic signature by FEA. Besides the requirements of efficient rotor position estimation in the whole-speed range, there are some challenging objectives for the design

of sensorless control, including high detection accuracy, high robustness, and improved algorithm versatility. To address these constraints, some advanced control theories, such as sliding mode observers and hybrid solutions that fuse multiple methods, are used for position estimation. Due to their excellent suitability for modeling nonlinear characteristics, reduced dependence on motor parameters and application in a wider speed range are expected in the future.

Author Contributions: Conceptualization, X.S. and M.Y.; methodology, X.T.; software, X.T.; validation, X.S., M.Y. and X.T.; formal analysis, M.Y.; writing—original draft preparation, X.T.; writing—review and editing, X.T.; visualization, X.S.; supervision, X.S.; project administration, M.Y.; funding acquisition, X.S. All authors have read and agreed to the published version of the manuscript.

Funding: This research received no external funding.

Institutional Review Board Statement: Not applicable.

Informed Consent Statement: Not applicable.

Data Availability Statement: The data set used in the current study will be made available on reasonable request.

Conflicts of Interest: The authors declare no conflict of interest.

References

1. Komatsuzaki, A.; Bamba, T.; Miki, I. Estimation of rotor position in a three-phase SRM at standstill and low speeds. *Electr. Eng. Jpn.* **2012**, *178*, 55–63. [\[CrossRef\]](#)
2. Sun, X.; Diao, K.; Lei, G.; Guo, Y.; Zhu, J. Real-Time HIL Emulation for a Segmented-Rotor Switched Reluctance Motor Using a New Magnetic Equivalent Circuit. *IEEE Trans. Power Electron.* **2020**, *35*, 3841–3849. [\[CrossRef\]](#)
3. Namazi, M.M.; Nezhad, S.M.S.; Tabesh, A.; Rashidi, A.; Liserre, M. Passivity-Based Control of Switched Reluctance-Based Wind System Supplying Constant Power Load. *IEEE Trans. Ind. Electron.* **2018**, *65*, 9550–9560. [\[CrossRef\]](#)
4. Wang, I.W.; Kim, Y.S. Rotor speed and position sensorless control of a switched reluctance motor using the binary observer. *IEE Proc.-Electr. Power Appl.* **2000**, *147*, 220–226.
5. Khalil, A.; Husain, I.; Hossain, S.; Gopalakrishnan, S.; Omekanda, A.; LeQuesne, B.; Klode, H. A hybrid sensorless SRM drive with eight- and six-switch converter topologies. *IEEE Trans. Ind. Appl.* **2004**, *41*, 1647–1655. [\[CrossRef\]](#)
6. Kosaka, T.; Matsui, N.; Saha, S.; Takeda, Y. Sensorless control of SRM based on a simple expression of magnetization characteristics. *Electr. Eng. Jpn.* **2001**, *137*, 52–60. [\[CrossRef\]](#)
7. Diao, K.; Sun, X.; Lei, G.; Guo, Y.; Zhu, J. Multiobjective System Level Optimization Method for Switched Reluctance Motor Drive Systems Using Finite-Element Model. *IEEE Trans. Ind. Electron.* **2020**, *67*, 10055–10064. [\[CrossRef\]](#)
8. Torkaman, H.; Afjei, E.; Toulabi, M.S. New Double-Layer-per-Phase Isolated Switched Reluctance Motor: Concept, Numerical Analysis, and Experimental Confirmation. *IEEE Trans. Ind. Electron.* **2012**, *59*, 830–838. [\[CrossRef\]](#)
9. Nezamabadi, M.M.; Afjei, E.; Torkaman, H. Design, Dynamic Electromagnetic Analysis, FEM, and Fabrication of a New Switched-Reluctance Motor with Hybrid Motion. *IEEE Trans. Magn.* **2015**, *52*, 1–8. [\[CrossRef\]](#)
10. Sato, Y.; Murakami, K.; Tsuboi, Y. Sensorless Torque and Thrust Estimation of a Rotational/Linear Two Degrees-of-Freedom Switched Reluctance Motor. *IEEE Trans. Magn.* **2016**, *52*, 1–4. [\[CrossRef\]](#)
11. Sun, X.; Diao, K.; Yang, Z. Performance improvement of a switched reluctance machine with segmental rotors for hybrid electric vehicles. *Comput. Electr. Eng.* **2019**, *77*, 244–259. [\[CrossRef\]](#)
12. Ma, B.-Y.; Liu, T.-H.; Chen, C.-G.; Shen, T.-J.; Feng, W.-S. Design and implementation of a sensorless switched reluctance drive system. *IEEE Trans. Aerosp. Electron. Syst.* **1998**, *34*, 1193–1207. [\[CrossRef\]](#)
13. Bartolo, J.B.; Degano, M.; Espina, J.; Gerada, C. Design and Initial Testing of a High-Speed 45-kW Switched Reluctance Drive for Aerospace Application. *IEEE Trans. Ind. Electron.* **2017**, *64*, 988–997. [\[CrossRef\]](#)
14. Li, J.-C.; Xin, M.; Fan, Z.-N.; Liu, R. Design and experimental evaluation of a 12 kw large synchronous reluctance motor and control system for elevator traction. *IEEE Access* **2020**, *8*, 34256–34264.
15. Wang, Q.; Jiang, W.; Jing, X.; Yu, Z. Sensorless Control of Segmented Bilateral Switched Reluctance Linear Motor Based on Coupled Voltage for Long Rail Propulsion Application. *IEEE Trans. Energy Convers.* **2020**, *35*, 1348–1359. [\[CrossRef\]](#)
16. Ullah, S.; McDonald, S.P.; Martin, R.; Benarous, M.; Atkinson, G.J. A Permanent Magnet Assist, Segmented Rotor, Switched Reluctance Drive for Fault Tolerant Aerospace Applications. *IEEE Trans. Ind. Appl.* **2019**, *55*, 298–305. [\[CrossRef\]](#)
17. Sun, X.; Xue, Z.; Han, S.; Chen, L.; Xu, X.; Yang, Z. Comparative study of fault-tolerant performance of a segmented rotor SRM and a conventional SRM. *Bull. Pol. Acad. Sci. Tech. Sci.* **2017**, *65*, 375–381. [\[CrossRef\]](#)
18. Ding, W.; Hu, Y.; Wu, L. Investigation and Experimental Test of Fault-Tolerant Operation of a Mutually Coupled Dual Three-Phase SRM Drive Under Faulty Conditions. *IEEE Trans. Power Electron.* **2015**, *30*, 6857–6872. [\[CrossRef\]](#)

19. Sun, Q.; Lan, T. Maximum Inductance Detection-based Fault-Tolerant Sensorless Control for SRM Drive. In Proceedings of the 2021 IEEE 4th Student Conference on Electric Machines and Systems (SCEMS), Huzhou, China, 1–3 December 2021; pp. 1–5.
20. Zhang, L.; Li, P. A fault tolerant sensorless techniques for switched reluctance motor. In Proceedings of the 2017 IEEE 3rd Information Technology and Mechatronics Engineering Conference (ITOEC), Chongqing, China, 3–5 October 2017; pp. 1243–1247.
21. Diao, K.; Sun, X.; Yao, M. Robust-Oriented Optimization of Switched Reluctance Motors Considering Manufacturing Fluctuation. *IEEE Trans. Transp. Electrification*. **2021**. [[CrossRef](#)]
22. Omekanda, A.M. Robust torque and torque-per-inertia optimization of a switched reluctance motor using the Taguchi methods. *IEEE Trans. Ind. Appl.* **2006**, *42*, 473–478. [[CrossRef](#)]
23. Fan, J.; Jung, I.; Lee, Y. Position Estimation of a Two-Phase Switched Reluctance Motor at Standstill. *Machines* **2021**, *9*, 359. [[CrossRef](#)]
24. Chen, H.; Yan, W.; Gu, J.J.; Sun, M. Multiobjective Optimization Design of a Switched Reluctance Motor for Low-Speed Electric Vehicles with a Taguchi–CSO Algorithm. *IEEE/ASME Trans. Mechatron.* **2018**, *23*, 1762–1774. [[CrossRef](#)]
25. Diao, K.; Sun, X.; Lei, G.; Bramerdorfer, G.; Guo, Y.; Zhu, J. System-Level Robust Design Optimization of a Switched Reluctance Motor Drive System Considering Multiple Driving Cycles. *IEEE Trans. Energy Convers.* **2021**, *36*, 348–357. [[CrossRef](#)]
26. de Paula, M.V.; dos Santos Barros, T.A. A Sliding Mode DITC Cruise Control for SRM with Steepest Descent Minimum Torque Ripple Point Tracking. *Trans. Ind. Electron.* **2022**, *69*, 151–159. [[CrossRef](#)]
27. Lin, F.-C.; Yang, S.-M. An Approach to Producing Controlled Radial Force in a Switched Reluctance Motor. *IEEE Trans. Ind. Electron.* **2007**, *54*, 2137–2146. [[CrossRef](#)]
28. Husain, I. Minimization of torque ripple in SRM drives. *IEEE Trans. Ind. Electron.* **2002**, *49*, 28–39. [[CrossRef](#)]
29. Lee, D.-H.; Liang, J.; Lee, Z.-G.; Ahn, J.-W. A Simple Nonlinear Logical Torque Sharing Function for Low-Torque Ripple SR Drive. *IEEE Trans. Ind. Electron.* **2009**, *56*, 3021–3028. [[CrossRef](#)]
30. Cai, J.; Zhao, X. Synthetic Hybrid-Integral-Threshold Logic-Based Position Fault Diagnosis Scheme for SRM Drives. *IEEE Trans. Instrum. Meas.* **2020**, *70*, 1–8. [[CrossRef](#)]
31. Ehsani, M.; Fahimi, B. Elimination of position sensors in switched reluctance motor drives: State of the art and future trends. *IEEE Trans. Ind. Electron.* **2002**, *49*, 40–47. [[CrossRef](#)]
32. Xue, X.D.; Cheng, K.W.E.; Ho, S.L.; Cheng, E.K.W. A Position Stepping Method for Predicting Performances of Switched Reluctance Motor Drives. *IEEE Trans. Energy Convers.* **2007**, *22*, 839–847. [[CrossRef](#)]
33. Han, S.; Liu, C.; Sun, X.; Diao, K. An effective method of verifying poles polarities in switched reluctance motors. *COMPEL—Int. J. Comput. Math. Electr. Electron. Eng.* **2019**, *38*, 927–938. [[CrossRef](#)]
34. Gallegos-Lopez, G.; Kjaer, P.; Miller, T. A new sensorless method for switched reluctance motor drives. *IEEE Trans. Ind. Appl.* **1998**, *34*, 832–840. [[CrossRef](#)]
35. Wang, W.; Fahimi, B. Fault Resilient Strategies for Position Sensorless Methods of Switched Reluctance Motors Under Single and Multiphase Fault. *IEEE J. Emerg. Sel. Top. Power Electron.* **2014**, *2*, 190–200. [[CrossRef](#)]
36. Ge, L.; Ralev, I.; Klein-Hessling, A.; Song, S.; De Doncker, R.W. A Simple Reluctance Calibration Strategy to Obtain the Flux-Linkage Characteristics of Switched Reluctance Machines. *IEEE Trans. Power Electron.* **2019**, *35*, 2787–2798. [[CrossRef](#)]
37. Chen, L.; Wang, H.; Sun, X.; Cai, Y.; Li, K.; Diao, K.; Wu, J. Development of digital control system for a belt-driven starter generator SSRM for HEVs. *Proc. Inst. Mech. Eng. Part I J. Syst. Control. Eng.* **2020**, *234*, 975–984.
38. Sun, X.; Wan, B.; Lei, G.; Tian, X.; Guo, Y.; Zhu, J. Multiobjective and Multiphysics Design Optimization of a Switched Reluctance Motor for Electric Vehicle Applications. *IEEE Trans. Energy Convers.* **2021**, *36*, 3294–3304. [[CrossRef](#)]
39. Mihic, D.S.; Terzic, M.; Vukosavic, S.N. A New Nonlinear Analytical Model of the SRM with Included Multiphase Coupling. *IEEE Trans. Energy Convers.* **2017**, *32*, 1322–1334. [[CrossRef](#)]
40. Sun, X.; Shen, Y.; Wang, S.; Lei, G.; Yang, Z.; Han, S. Core losses analysis of a novel 16/10 segmented rotor switched reluctance BSG motor for HEVs using nonlinear lumped parameter equivalent circuit model. *IEEE/ASME Trans. Mechatron.* **2018**, *23*, 747–757. [[CrossRef](#)]
41. Pillay, P.; Ahmed, M.; Samudio, M. Modeling and performance of a SRM drive with improved ride-through capability. *IEEE Trans. Energy Convers.* **2001**, *16*, 165–173. [[CrossRef](#)]
42. Liang, Y.; Chen, H. Circuit-based flux linkage measurement method with the automated resistance correction for SRM sensorless position control. *IET Electr. Power Appl.* **2018**, *12*, 1396–1406. [[CrossRef](#)]
43. Sun, X.; Wu, J.; Lei, G.; Cai, Y.; Chen, X.; Guo, Y. Torque Modeling of a Segmented-Rotor SRM Using Maximum-Correntropy-Criterion-Based LSSVR for Torque Calculation of EVs. *IEEE J. Emerg. Sel. Top. Power Electron.* **2021**, *9*, 2674–2684. [[CrossRef](#)]
44. Radimov, N.; Ben-Hail, N.; Rabinovici, R. Simple Model of Switched-Reluctance Machine Based only on Aligned and Unaligned Position Data. *IEEE Trans. Magn.* **2004**, *40*, 1562–1572. [[CrossRef](#)]
45. Ralev, I.; Max, S.; De Doncker, R.W. Accurate Rotor Position Detection for Low-Speed Operation of Switched Reluctance Drives. In Proceedings of the 2018 IEEE 18th International Power Electronics and Motion Control Conference (PEMC), Budapest, Hungary, 26–30 August 2018; pp. 483–490.
46. Gan, C.; Wu, J.; Wang, N.; Hu, Y.; Cao, W.; Yang, S. Independent Current Control of Dual Parallel SRM Drive Using a Public Current Sensor. *IEEE/ASME Trans. Mechatron.* **2017**, *22*, 392–401. [[CrossRef](#)]
47. Li, X.; Shamsi, P. Model Predictive Current Control of Switched Reluctance Motors with Inductance Auto-Calibration. *IEEE Trans. Ind. Electron.* **2016**, *63*, 3934–3941. [[CrossRef](#)]

48. Fang, G.; Scalcon, F.P.; Xiao, D.; Vieira, R.P.; Grundling, H.A.; Emadi, A. Advanced Control of Switched Reluctance Motors (SRMs): A Review on Current Regulation, Torque Control and Vibration Suppression. *IEEE Open J. Ind. Electron. Soc.* **2021**, *2*, 280–301. [[CrossRef](#)]
49. Alharkan, H.; Saadatmand, S.; Ferdowsi, M.; Shamsi, P. Optimal Tracking Current Control of Switched Reluctance Motor Drives Using Reinforcement Q-Learning Scheduling. *IEEE Access* **2021**, *9*, 9926–9936. [[CrossRef](#)]
50. Shao, W.; Zhong, R.; Guo, X.; Sun, W. Analysis of the null current gradient position for sensorless control of SRM. In Proceedings of the IECON 2017—43rd Annual Conference of the IEEE Industrial Electronics Society, Beijing, China, 29 October–1 November 2017; pp. 1816–1821. [[CrossRef](#)]
51. Dankadai, N.K.; Elgendy, M.A.; McDonald, S.P.; Atkinson, D.J.; Hasaniien, H.M. Model-Based Sensorless Torque Control of SRM Drive Using Single Current Sensor. In Proceedings of the 10th International Conference on Power Electronics, Machines and Drives (PEMD 2020), Online Conference, 15–17 December 2020; pp. 960–965.
52. Sun, X.; Wu, J.; Lei, G.; Guo, Y.; Zhu, J. Torque Ripple Reduction of SRM Drive Using Improved Direct Torque Control with Sliding Mode Controller and Observer. *IEEE Trans. Ind. Electron.* **2020**, *68*, 9334–9345. [[CrossRef](#)]
53. Wang, H.; Chen, L.; Sun, X.; Cai, Y.; Diao, K. Design optimization and analysis of a segmented-rotor switched reluctance machine for BSG application in HEVs. *Int. J. Appl. Electromagn. Mech.* **2020**, *63*, 529–550. [[CrossRef](#)]
54. Li, Z.; Hu, B.; Li, C.; Lee, D.-H.; Ahn, J.-W. SRM sensorless speed control based on the improved simplified flux method. In Proceedings of the 2011 International Conference on Electrical Machines and Systems, Beijing, China, 20–23 August 2011; pp. 1–4.
55. Pupadubsin, R.; Mecrow, B.C.; Widmer, J.D.; Steven, A. Smooth Voltage PWM for Vibration and Acoustic Noise Reduction in Switched Reluctance Machines. *IEEE Trans. Energy Convers.* **2020**, *36*, 1578–1588. [[CrossRef](#)]
56. Mthombeni, T.L.; Pillay, P. Lamination core losses in motors with nonsinusoidal excitation with particular reference to PWM and SRM excitation waveforms. *IEEE Trans. Energy Convers.* **2005**, *20*, 836–843. [[CrossRef](#)]
57. Xu, S.; Chen, H.; Dong, F.; Yang, J. Reliability Analysis on Power Converter of Switched Reluctance Machine System under Different Control Strategies. *IEEE Trans. Ind. Electron.* **2019**, *66*, 6570–6580. [[CrossRef](#)]
58. Sun, X.; Feng, L.; Zhu, Z.; Lei, G.; Diao, K.; Guo, Y.; Zhu, J. Optimal Design of Terminal Sliding Mode Controller for Direct Torque Control of SRMs. *IEEE Trans. Transp. Electrif.* **2021**, *8*, 1445–1453. [[CrossRef](#)]
59. Yao, S.; Zhang, W. A Simple Strategy for Parameters Identification of SRM Direct Instantaneous Torque Control. *IEEE Trans. Power Electron.* **2017**, *33*, 3622–3630. [[CrossRef](#)]
60. Ye, J.; Bilgin, B.; Emadi, A. An Offline Torque Sharing Function for Torque Ripple Reduction in Switched Reluctance Motor Drives. *IEEE Trans. Energy Convers.* **2015**, *30*, 726–735. [[CrossRef](#)]
61. Li, H.; Bilgin, B.; Emadi, A. An Improved Torque Sharing Function for Torque Ripple Reduction in Switched Reluctance Machines. *IEEE Trans. Power Electron.* **2019**, *34*, 1635–1644. [[CrossRef](#)]
62. Xia, Z.; Bilgin, B.; Nalakath, S.; Emadi, A. A New Torque Sharing Function Method for Switched Reluctance Machines with Lower Current Tracking Error. *IEEE Trans. Ind. Electron.* **2020**, *68*, 10612–10622. [[CrossRef](#)]
63. Ehsani, M.; Mahajan, S.; Ramani, K.; Husain, I. New modulation encoding techniques for indirect rotor position sensing in switched reluctance motors. *IEEE Trans. Ind. Appl.* **1994**, *30*, 85–91. [[CrossRef](#)]
64. Ge, L.; Xu, H.; Guo, Z.; Song, S.; De Doncker, R.W. An Optimization-Based Initial Position Estimation Method for Switched Reluctance Machines. *IEEE Trans. Power Electron.* **2021**, *36*, 13285–13292. [[CrossRef](#)]
65. Al-Bahadly, I.H. Examination of a Sensorless Rotor-Position-Measurement Method for Switched Reluctance Drive. *IEEE Trans. Ind. Electron.* **2008**, *55*, 288–295. [[CrossRef](#)]
66. Gallegos-Lopez, G.; Kjaer, P.; Miller, T. High-grade position estimation for SRM drives using flux linkage/current correction model. *IEEE Trans. Ind. Appl.* **1999**, *35*, 859–869. [[CrossRef](#)]
67. Song, S.; Chen, S.; Liu, W. Analytical Rotor Position Estimation for SRM Based on Scaling of Reluctance Characteristics from Torque-Balanced Measurement. *IEEE Trans. Ind. Electron.* **2016**, *64*, 3524–3536. [[CrossRef](#)]
68. Song, S.; Zhang, M.; Ge, L. A New Decoupled Analytical Modeling Method for Switched Reluctance Machine. *IEEE Trans. Magn.* **2015**, *51*, 1–4. [[CrossRef](#)]
69. Sheth, N.K.; Rajagopal, K.R. Calculation of the flux-linkage characteristics of a switched reluctance motor by flux tube method. *IEEE Trans. Magn.* **2005**, *41*, 4069–4071. [[CrossRef](#)]
70. Sun, X.; Zhou, Z.; Chen, L.; Yang, Z.; Han, S. Performance analysis of segmented rotor switched reluctance motors with three types of winding connections for belt-driven starter generators of hybrid electric vehicles. *COMPEL Int. J. Comput. Mathemat. Electri. Electron. Engin.* **2018**, *37*, 1258–1270. [[CrossRef](#)]
71. Chang, Y.; Cheng, K.W.E. Sensorless position estimation of switched reluctance motor at startup using quadratic polynomial regression. *IET Electr. Power Appl.* **2013**, *7*, 618–626. [[CrossRef](#)]
72. Chang, Y.-T.; Cheng, E.K.W.; Ho, S.L. Type-V Exponential Regression for Online Sensorless Position Estimation of Switched Reluctance Motor. *IEEE/ASME Trans. Mechatron.* **2015**, *20*, 1351–1359. [[CrossRef](#)]
73. Ye, J.; Bilgin, B.; Emadi, A. Elimination of Mutual Flux Effect on Rotor Position Estimation of Switched Reluctance Motor Drives Considering Magnetic Saturation. *IEEE Trans. Power Electron.* **2015**, *30*, 532–536. [[CrossRef](#)]
74. Salmasi, F.; Fahimi, B. Modeling Switched-Reluctance Machines by Decomposition of Double Magnetic Saliencies. *IEEE Trans. Magn.* **2004**, *40*, 1556–1561. [[CrossRef](#)]

75. Fahimi, B.; Emadi, A.; Sepe, R. Four-Quadrant Position Sensorless Control in SRM Drives Over the Entire Speed Range. *IEEE Trans. Power Electron.* **2005**, *20*, 154–163. [[CrossRef](#)]
76. Ding, W.; Song, K. Position Sensorless Control of Switched Reluctance Motors Using Reference and Virtual Flux Linkage with One-Phase Current Sensor in Medium and High Speed. *IEEE Trans. Ind. Electron.* **2019**, *67*, 2595–2606. [[CrossRef](#)]
77. Peng, F.; Ye, J.; Emadi, A.; Huang, Y. Position Sensorless Control of Switched Reluctance Motor Drives Based on Numerical Method. *IEEE Trans. Ind. Appl.* **2017**, *53*, 2159–2168. [[CrossRef](#)]
78. Zhang, X.; Tan, G.; Kuai, S.; Wang, Q. Position Sensorless Control of Switched Reluctance Generator for Wind Energy Conversion. In Proceedings of the 2010 Asia-Pacific Power and Energy Engineering Conference, Chengdu, China, 28–31 March 2010; pp. 1–5.
79. Xiao, D.; Ye, J.; Fang, G.; Xia, Z.; Emadi, A. Magnetic-Characteristic-Free High-Speed Position-Sensorless Control of Switched Reluctance Motor Drives with Quadrature Flux Estimators. *IEEE J. Emerg. Sel. Top. Power Electron.* **2021**, *10*, 220–235. [[CrossRef](#)]
80. Wei, W.; Wang, Q.; Nie, R. Sensorless control of double-sided linear switched reluctance motor based on simplified flux linkage method. *CES Trans. Electr. Mach. Syst.* **2017**, *1*, 246–253. [[CrossRef](#)]
81. Cheok, A.D.; Wang, Z. DSP-Based Automated Error-Reducing Flux-Linkage-Measurement Method for Switched Reluctance Motors. *IEEE Trans. Instrum. Meas.* **2007**, *56*, 2245–2253. [[CrossRef](#)]
82. Zhang, Y.; Liu, C.; Zhang, L. Sensorless control of SRM based on improved simplified flux-linkage method. In Proceedings of the 2014 17th International Conference on Electrical Machines and Systems (ICEMS), Hangzhou, China, 22–25 October 2014; Volume 1, pp. 722–726.
83. Song, S.; Ge, L.; Zhang, Z. Accurate Position Estimation of SRM Based on Optimal Interval Selection and Linear Regression Analysis. *IEEE Trans. Ind. Electron.* **2016**, *63*, 3467–3478. [[CrossRef](#)]
84. Wang, T.; Ding, W.; Hu, Y.; Yang, S.; Li, S. Sensorless control of switched reluctance motor drive using an improved simplified flux linkage model method. In Proceedings of the 2018 IEEE Applied Power Electronics Conference and Exposition (APEC), San Antonio, TX, USA, 4–8 March 2018; pp. 2992–2998.
85. Xu, A.; Chen, J.; Ren, P.; Zhu, J. Position sensorless control of switched reluctance motor based on a linear inductance model with variable coefficients. *IET Energy Syst. Integr.* **2019**, *1*, 210–217. [[CrossRef](#)]
86. Ha, K.; Kim, R.-Y.; Ramu, R. Position estimation in switched reluctance motor drives using the first switching Harmonics through Fourier series. *IEEE Trans. Ind. Electron.* **2011**, *58*, 5352–5360. [[CrossRef](#)]
87. Kim, J.; Lai, J.-S. Quad sampling incremental inductance measurement through current loop for switched reluctance motor. *IEEE Trans. Instrum. Meas.* **2020**, *69*, 4251–4257. [[CrossRef](#)]
88. Gan, C.; Meng, F.; Yu, Z.; Qu, R.; Liu, Z.; Si, J. Online Calibration of Sensorless Position Estimation for Switched Reluctance Motors with Parametric Uncertainties. *IEEE Trans. Power Electron.* **2020**, *35*, 12307–12320. [[CrossRef](#)]
89. Kuai, S.; Zhao, S.; Heng, F.; Cui, X. Position sensorless technology of switched reluctance motor drives including mutual inductance. *IET Electr. Power Appl.* **2017**, *11*, 1085–1094. [[CrossRef](#)]
90. Ge, L.; Zhong, J.; Bao, C.; Song, S.; De Doncker, R.W. Continuous Rotor Position Estimation for SRM Based on Transformed Unsaturated Inductance Characteristic. *IEEE Trans. Power Electron.* **2021**, *37*, 37–41. [[CrossRef](#)]
91. Cai, H.; Wang, H.; Li, M.; Shen, S.; Feng, A.Y. Position Sensorless Control of Switched Reluctance Motor with Consideration of Magnetic Saturation Based on Phase-Inductance Intersection Points Information. *Energies* **2018**, *11*, 3517. [[CrossRef](#)]
92. Gao, H.; Salmasi, F.R.; Ehsani, M. Inductance Model-Based Sensorless Control of the Switched Reluctance Motor Drive at Low Speed. *IEEE Trans. Power Electron.* **2004**, *19*, 1568–1573. [[CrossRef](#)]
93. Cai, J.; Deng, Z. Sensorless Control of Switched Reluctance Motor Based on Phase Inductance Vectors. *IEEE Trans. Power Electron.* **2012**, *27*, 3410–3423. [[CrossRef](#)]
94. Sun, X.; Tang, X.; Tian, X.; Lei, G.; Guo, Y.; Zhu, J. Sensorless Control with Fault-Tolerant Ability for Switched Reluctance Motors. *IEEE Trans. Energy Convers.* **2021**. [[CrossRef](#)]
95. Cai, J.; Deng, Z.; Hu, R. Position Signal Faults Diagnosis and Control for Switched Reluctance Motor. *IEEE Trans. Magn.* **2014**, *50*, 1–11. [[CrossRef](#)]
96. Cai, J.; Deng, Z. Initial Rotor Position Estimation and Sensorless Control of SRM Based on Coordinate Transformation. *IEEE Trans. Instrum. Meas.* **2014**, *64*, 1004–1018. [[CrossRef](#)]
97. Cai, J.; Liu, Z. An Unsaturated Inductance Reconstruction Based Universal Sensorless Starting Control Scheme for SRM Drives. *IEEE Trans. Ind. Electron.* **2020**, *67*, 9083–9092. [[CrossRef](#)]
98. Cai, J.; Deng, Z. Unbalanced Phase Inductance Adaptable Rotor Position Sensorless Scheme for Switched Reluctance Motor. *IEEE Trans. Power Electron.* **2017**, *33*, 4285–4292. [[CrossRef](#)]
99. Kim, J.H.; Kim, R.-Y. Sensorless direct torque control using the inductance inflection point for a switched reluctance motor. *IEEE Trans. Ind. Electron.* **2018**, *65*, 9336–9345. [[CrossRef](#)]
100. Miki, I.; Noda, H.; Moriyama, R. A sensorless drive method for switched reluctance motor based on gradient of phase inductance. In Proceedings of the 6th International Conference on Electrical Machines and Systems (ICEMS), Beijing, China, 9–11 November 2003; Volume 2, pp. 615–618.
101. Cai, J.; Liu, Z.; Zeng, Y. Aligned Position Estimation Based Fault-Tolerant Sensorless Control Strategy for SRM Drives. *IEEE Trans. Power Electron.* **2018**, *34*, 7754–7762. [[CrossRef](#)]
102. Torkaman, H.; Afjei, E.; Babaee, H.; Yadegari, P. Novel Method of ACO and Its Application to Rotor Position Estimation in a SRM under Normal and Faulty Conditions. *J. Power Electron.* **2011**, *11*, 856–863. [[CrossRef](#)]

103. Murugan, L.S.; Maruthupandi, P. Sensorless speed control of 6/4-pole switched reluctance motor with ANFIS and fuzzy-PID-based hybrid observer. *Electr. Eng.* **2020**, *102*, 831–844. [[CrossRef](#)]
104. Cheok, A.; Ertugrul, N. High robustness and reliability of fuzzy logic based position estimation for sensorless switched reluctance motor drives. *IEEE Trans. Power Electron.* **2000**, *15*, 319–334. [[CrossRef](#)]
105. Cheok, A.; Wang, Z. Fuzzy Logic Rotor Position Estimation Based Switched Reluctance Motor DSP Drive with Accuracy Enhancement. *IEEE Trans. Power Electron.* **2005**, *20*, 908–921. [[CrossRef](#)]
106. de Araujo Porto Henriques, L.O.; Rolim, L.G.B.; Suemitsu, W.I.; Dente, J.A.; Branco, P. Development and Experimental Tests of a Simple Neurofuzzy Learning Sensorless Approach for Switched Reluctance Motors. *IEEE Trans. Power Electron.* **2011**, *26*, 3330–3344. [[CrossRef](#)]
107. Wu, J.; Sun, X.; Zhu, J. Accurate torque modeling with PSO-based recursive robust LSSVR for a segmented-rotor switched reluctance motor. *CES Trans. Electr. Mach. Syst.* **2020**, *4*, 96–104. [[CrossRef](#)]
108. Mese, E.; Torrey, D.A. Sensorless position estimation for variable-reluctance machines using artificial neural networks. In Proceedings of the IAS '97. Conference Record of the 1997 IEEE Industry Applications Conference Thirty-Second IAS Annual Meeting, New Orleans, LA, USA, 5–9 October 1997; pp. 540–547.
109. Mese, E.; Torrey, D. An approach for sensorless position estimation for switched reluctance motors using artificial neural networks. *IEEE Trans. Power Electron.* **2002**, *17*, 66–75. [[CrossRef](#)]
110. Paramasivam, S.; Vijayan, S.; Vasudevan, M.; Arumugam, R.; Krishnan, R. Real-time verification of AI based rotor position estimation techniques for a 6/4 pole switched reluctance motor drive. *IEEE Trans. Magn.* **2007**, *43*, 3209–3222. [[CrossRef](#)]
111. Zhou, Y.; Xia, C.; He, Z.; Xie, X. Torque Ripple Minimization in a Sensorless Switched Reluctance Motor Based on Flexible Neural Networks. In Proceedings of the 2007 IEEE International Conference on Control and Automation, Guangzhou, China, 30 May–1 June 2007; pp. 2340–2344.
112. Hudson, C.; Lobo, N.; Krishnan, R. Sensorless control of single switch based switched reluctance motor drive using neural network. *IEEE Trans. Ind. Electron.* **2008**, *55*, 321–329. [[CrossRef](#)]
113. Cai, Y.; Wang, Y.; Xu, H.; Sun, S.; Wang, C.; Sun, L. Research on rotor position model for switched reluctance motor using neural network. *IEEE/ASME Trans. Mechatron.* **2018**, *23*, 2762–2773.
114. Capecchi, E.; Guglielmi, P.; Pastorelli, M.; Vagati, A. Position-sensorless control of the transverse-laminated synchronous reluctance motor. *IEEE Trans. Ind. Appl.* **2001**, *37*, 1768–1776. [[CrossRef](#)]
115. Abdelmaksoud, H.; Zaky, M. Design of an Adaptive Flux Observer for Sensorless Switched Reluctance Motors Using Lyapunov Theory. *Adv. Electr. Comput. Eng.* **2020**, *20*, 123–130. [[CrossRef](#)]
116. Elmas, Ç.; La Parra, H.Z.-D. Application of a full-order extended Luenberger observer for a position sensorless operation of a switched reluctance motor drive. *IEE Proc.-Control. Theory Appl.* **1996**, *143*, 401–408. [[CrossRef](#)]
117. Islam, M.; Husain, J. Torque-ripple minimization with indirect position and speed sensing for switched reluctance motors. *IEEE Trans. Ind. Electron.* **2000**, *47*, 1126–1133. [[CrossRef](#)]
118. Sun, X.; Feng, L.; Diao, K.; Yang, Z. An Improved Direct Instantaneous Torque Control Based on Adaptive Terminal Sliding Mode for a Segmented-Rotor SRM. *IEEE Trans. Ind. Electron.* **2020**, *68*, 10569–10579. [[CrossRef](#)]
119. Brandstetter, P.; Petrtyl, O.; Hajovsky, J. Luenberger observer application in control of switched reluctance motor. In Proceedings of the 2016 17th International Scientific Conference on Electric Power Engineering (EPE), Prague, Czech Republic, 16–18 May 2016; pp. 1–5.
120. Zhan, Y.; Chan, C.; Chau, K. A novel position and velocity observer for robust control of switched reluctance motors. In Proceedings of the 29th Annual IEEE Power Electronics Specialists Conference, Fukuoka, Japan, 22 May 1998; Volume 2, pp. 1315–1321.
121. McCann, R.A.; Islam, M.S.; Husain, I. Application of a sliding-mode observer for position and speed estimation in switched reluctance motor drives. *IEEE Trans. Ind. Appl.* **2001**, *37*, 51–58. [[CrossRef](#)]
122. Zhan, Y.; Chan, C.; Chau, K. A novel sliding-mode observer for indirect position sensing of switched reluctance motor drives. *IEEE Trans. Ind. Electron.* **1999**, *46*, 390–397. [[CrossRef](#)]
123. Khalil, A.; Underwood, S.; Husain, I.; Klode, H.; LeQuesne, B.; Gopalakrishnan, S.; Omekanda, A.M. Four-Quadrant Pulse Injection and Sliding-Mode-Observer-Based Sensorless Operation of a Switched Reluctance Machine over Entire Speed Range Including Zero Speed. *IEEE Trans. Ind. Appl.* **2007**, *43*, 714–723. [[CrossRef](#)]
124. Yalavarthi, A.; Singh, B. SMO-Based Position Sensorless SRM Drive for Battery Supported PV Submersible Pumps. *IEEE J. Emerg. Sel. Top. Power Electron.* **2021**. [[CrossRef](#)]
125. Sun, X.; Tang, X.; Tian, X.; Wu, J.; Zhu, J. Position Sensorless Control of Switched Reluctance Motor Drives Based on a New Sliding Mode Observer Using Fourier Flux Linkage Model. *IEEE Trans. Energy Convers.* **2021**. [[CrossRef](#)]
126. Sun, J.; Cao, G.-Z.; Huang, S.-D.; Peng, Y.; He, J.; Qian, Q.-Q. Sliding-Mode-Observer-Based Position Estimation for Sensorless Control of the Planar Switched Reluctance Motor. *IEEE Access* **2019**, *7*, 61034–61045. [[CrossRef](#)]
127. Xu, L.; Wang, C. Accurate rotor position detection and sensorless control of SRM for super-high speed operation. *IEEE Trans. Power Electron.* **2002**, *17*, 757–763. [[CrossRef](#)]
128. Xiao, D.; Ye, J.; Fang, G.; Xia, Z.; Wang, X.; Emadi, A. Improved Feature-Position-Based Sensorless Control Scheme for SRM Drives Based on Nonlinear State Observer at Medium and High Speeds. *IEEE Trans. Power Electron.* **2021**, *36*, 5711–5723. [[CrossRef](#)]

129. Pasquesoone, G.; Mikail, R.; Husain, I. Position estimation at starting and lower speed in three-phase switched reluctance machines using pulse injection and two thresholds. *IEEE Trans. Ind. Appl.* **2011**, *47*, 1724–1731. [[CrossRef](#)]
130. Daldaban, F.; Buzpinar, M.A. Pulse injection-based sensorless switched reluctance motor driver model with machine learning algorithms. *Electr. Eng.* **2021**, *103*, 705–715. [[CrossRef](#)]
131. Ofori, E.; Husain, T.; Sozer, Y.; Husain, I. A pulse injection based sensorless position estimation method for a switched reluctance machine over a wide speed range. *IEEE Trans. Ind. Appl.* **2015**, *51*, 3867–3876. [[CrossRef](#)]
132. Kim, J.; Choe, J.-M.; Moon, S.; Lai, J.-S. Position Sensorless Control of Switched Reluctance Motor Drives without Pre-stored Magnetic Characteristics. In Proceedings of the 2018 IEEE Energy Conversion Congress and Exposition (ECCE), Portland, OR, USA, 23–27 September 2018; pp. 1755–1761.
133. Cai, J.; Yan, Y.; Zhang, W.; Zhao, X. A Reliable Sensorless Starting Scheme for SRM with Lowered Pulse Injection Current Influences. *IEEE Trans. Instrum. Meas.* **2021**, *70*, 1–9. [[CrossRef](#)]
134. Xiao, D.; Ye, J.; Fang, G.; Xia, Z.; Wang, X.; Emadi, A. A Regional Phase-Locked Loop-Based Low-Speed Position-Sensorless Control Scheme for General-Purpose Switched Reluctance Motor Drives. *IEEE Trans. Power Electron.* **2021**, *37*, 5859–5873. [[CrossRef](#)]
135. Shi, T.; Cao, Y.; Jiang, G.; Li, X.; Xia, C. A Torque Control Strategy for Torque Ripple Reduction of Brushless DC Motor With Nonideal Back Electromotive Force. *IEEE Trans. Ind. Electron.* **2017**, *64*, 4423–4433. [[CrossRef](#)]
136. Hu, K.-W.; Chen, Y.-Y.; Liaw, C.-M. A Reversible Position Sensorless Controlled Switched-Reluctance Motor Drive with Adaptive and Intuitive Commutation Tunings. *IEEE Trans. Power Electron.* **2014**, *30*, 3781–3793. [[CrossRef](#)]
137. Bu, J.; Xu, L. Eliminating starting hesitation for reliable sensorless control of switched reluctance motors. *IEEE Trans. Ind. Appl.* **2001**, *37*, 59–66.
138. Krishnamurthy, M.; Edrington, C.; Fahimi, B. Prediction of rotor position at standstill and rotating shaft conditions in switched reluctance machines. *IEEE Trans. Power Electron.* **2006**, *21*, 225–233. [[CrossRef](#)]
139. Geldhof, K.R.; Van den Bossche, A.P.M.; Melkebeek, J.A. Rotor-Position Estimation of Switched Reluctance Motors Based on Damped Voltage Resonance. *IEEE Trans. Ind. Electron.* **2009**, *57*, 2954–2960. [[CrossRef](#)]
140. Shen, L.; Wu, J.; Yang, S. Initial Position Estimation in SRM Using Bootstrap Circuit without Predefined Inductance Parameters. *IEEE Trans. Power Electron.* **2011**, *26*, 2449–2456. [[CrossRef](#)]
141. Yoon, Y.-H. A Study of Rotor Position Detection and Control through Low-Cost Circuit Design of SRM. *J. Electr. Eng. Technol.* **2021**, *16*, 2817–2827. [[CrossRef](#)]
142. Cai, J.; Liu, Z.; Zeng, Y.; Jia, H.; Deng, Z. A Hybrid-Harmonic-Filter-Based Position Estimation Method for an SRM with Embedded Inductive Sensing Coils. *IEEE Trans. Power Electron.* **2018**, *33*, 10602–10610. [[CrossRef](#)]
143. Consoli, A.; Russo, F.; Scarcella, G.; Testa, A. Low- and zero-speed sensorless control of synchronous reluctance motors. *IEEE Trans. Ind. Appl.* **1999**, *35*, 1050–1057. [[CrossRef](#)]
144. Chen, H.; Nie, R.; Gu, J.; Yan, S.; Zhao, R. Efficiency Optimization Strategy for Switched Reluctance Generator System with Position Sensorless Control. *IEEE/ASME Trans. Mechatron.* **2021**, *26*, 469–479. [[CrossRef](#)]
145. Hossain, S.; Husain, I.; Klode, H.; Omekanda, A.; Gopalakrishan, S. Four quadrant and zero speed sensorless control of a switched reluctance motor. *IEEE Trans. Ind. Appl.* **2003**, *39*, 1343–1349. [[CrossRef](#)]
146. Kim, S.; Kim, J.-H.; Kimf, R.-Y. Sensor-less direct torque control using inductance peak detection for switched reluctance motor. In Proceedings of the 2015 IEEE Conference on Energy Conversion (CENCON), Johor Bahru, Malaysia, 19–20 October 2015; pp. 7–12.
147. Bateman, C.J.; Mecrow, B.C.; Clothier, A.C.; Acarnley, P.P.; Tuftnell, N.D. Sensorless Operation of an Ultra-High-Speed Switched Reluctance Machine. *IEEE Trans. Ind. Appl.* **2010**, *46*, 2329–2337. [[CrossRef](#)]
148. Cai, J.; Deng, Z. A Joint Feature Position Detection-Based Sensorless Position Estimation Scheme for Switched Reluctance Motors. *IEEE Trans. Ind. Electron.* **2017**, *64*, 4352–4360. [[CrossRef](#)]
149. Gan, C.; Wu, J.; Hu, Y.; Yang, S.; Cao, W.; Kirtley, J.L. Online Sensorless Position Estimation for Switched Reluctance Motors Using One Current Sensor. *IEEE Trans. Power Electron.* **2015**, *31*, 1. [[CrossRef](#)]
150. Husain, T.; Elrayah, A.; Sozer, Y.; Husain, I. Unified Control for Switched Reluctance Motors for Wide Speed Operation. *IEEE Trans. Ind. Electron.* **2019**, *66*, 3401–3411. [[CrossRef](#)]
151. Kioskeridis, I.; Mademlis, C. A Unified Approach for Four-Quadrant Optimal Controlled Switched Reluctance Machine Drives with Smooth Transition Between Control Operations. *IEEE Trans. Power Electron.* **2008**, *24*, 301–306. [[CrossRef](#)]
152. Diao, K.; Sun, X.; Chen, L.; Cai, Y.; Wang, H.; Wu, J. Direct Torque Control of A Segmented Switched Reluctance Motor for BSG in HEVs. In Proceedings of the 2019 3rd Conference on Vehicle Control and Intelligence (CVCI), Hefei, China, 21–22 September 2019; pp. 1–6.
153. Yang, H.-Y.; Kim, J.-H.; Krishnan, R. Low-Cost Position Sensorless Switched Reluctance Motor Drive Using a Single-Controllable Switch Converter. *J. Power Electron.* **2012**, *12*, 75–82. [[CrossRef](#)]
154. Feng, L.; Sun, X.; Tian, X.; Diao, K. Direct Torque Control with Variable Flux for an SRM Based on Hybrid Optimization Algorithm. *IEEE Trans. Power Electron.* **2022**, *37*, 6688–6697. [[CrossRef](#)]
155. Shao, J.; Deng, Z.; Gu, Y. Fault-Tolerant Control of Position Signals for Switched Reluctance Motor Drives. *IEEE Trans. Ind. Appl.* **2017**, *53*, 2959–2966. [[CrossRef](#)]

156. Pinto, D.; Pelletier, J.; Peng, W.; Gyselinck, J. Combined Signal-Injection and Flux-Linkage Approach for Sensorless Control of Switched Reluctance Machines. In Proceedings of the 2016 IEEE Vehicle Power and Propulsion Conference (VPPC), Hangzhou, China, 17–20 October 2016; pp. 1–6.
157. Yousefi-Talouki, A.; Pescetto, P.; Pellegrino, G.-M.L.; Boldea, I. Combined Active Flux and High-Frequency Injection Methods for Sensorless Direct-Flux Vector Control of Synchronous Reluctance Machines. *IEEE Trans. Power Electron.* **2018**, *33*, 2447–2457. [[CrossRef](#)]
158. Divandari, M.; Rezaie, B.; Noei, A.R. Sensorless drive for switched reluctance motor by adaptive hybrid sliding mode observer without chattering. In Proceedings of the 2018 IEEE Conference of Russian Young Researchers in Electrical and Electronic Engineering (EIConRus), Saint Petersburg, Russia, 29 January–1 February 2018; Volume 2018, pp. 1714–1722.
159. Kim, J.; Kim, R. Online sensorless position estimation for switched reluctance motors using characteristics of overlap position based on inductance profile. *IET Electr. Power Appl.* **2019**, *13*, 456–462. [[CrossRef](#)]
160. Gan, C.; Chen, Y.; Sun, Q.; Si, J.; Wu, J.; Hu, Y. A Position Sensorless Torque Control Strategy for Switched Reluctance Machines with Fewer Current Sensors. *IEEE/ASME Trans. Mechatron.* **2021**, *26*, 1118–1128. [[CrossRef](#)]
161. Sahoo, S.K.; Dasgupta, S.; Panda, S.K.; Xu, J.-X. A Lyapunov function-based robust direct torque controller for a switched reluctance motor drive system. *IEEE Trans. Power Electron.* **2012**, *27*, 555–564. [[CrossRef](#)]
162. Sun, X.; Diao, K.; Lei, G.; Guo, Y.; Zhu, J. Direct Torque Control Based on a Fast Modeling Method for a Segmented-Rotor Switched Reluctance Motor in HEV Application. *IEEE J. Emerg. Sel. Top. Power Electron.* **2021**, *9*, 232–241. [[CrossRef](#)]
163. Gong, C.; Li, S.; Habetler, T.; Restrepo, J.A.; Soderholm, B. Direct Position Control for Ultrahigh-Speed Switched-Reluctance Machines Based on Low-Cost Nonintrusive Reflective Sensors. *IEEE Trans. Ind. Appl.* **2018**, *55*, 480–489. [[CrossRef](#)]
164. Ehsani, M.; Husain, I. Rotor position sensing in switched reluctance motor drives by measuring mutually induced voltages. *IEEE Trans. Ind. Appl.* **1994**, *30*, 665–672. [[CrossRef](#)]
165. Panda, D.; Ramanarayanan, V. Mutual Coupling and Its Effect on Steady-State Performance and Position Estimation of Even and Odd Number Phase Switched Reluctance Motor Drive. *IEEE Trans. Magn.* **2007**, *43*, 3445–3456. [[CrossRef](#)]
166. Zhou, D.; Chen, H. Four-Quadrant Position Sensorless Operation of Switched Reluctance Machine for Electric Vehicles over a Wide Speed Range. *IEEE Trans. Transp. Electrification.* **2021**, *7*, 2835–2847. [[CrossRef](#)]